Journal of Structural Geology, Vol. 4, No. 3, pp. 257 to 269, 1982
Printed in Great Britain

0191-8141/82/030257-13 $03.00/0

Cataclasites along the Saltville thrust, U.S.A. and their implications for thrust-sheet emplacement

WILLIAM M. HOUSE* and DAVID R. GRAY

Department of Geological Sciences, Virginia Polytechnic Institute and State University, Blacksburg, VA 24061, U.S.A.

(*Received* 26 *May* 1981; *accepted in revised form* 19 *April* 1982)

Abstract—Cataclasis and frictional wear are the primary bulk deformation mechanisms along steeply dipping portions of the Saltville thrust in the southern Appalachian foreland zone, U.S.A. Fault character ranges from a single discrete sliding surface with negligible gouge, to a zone of several discrete sliding surfaces or a zone (up to 0.3 m thick) of pervasive cataclasite. Marked fracturing occurs up to 20 m above the fault, whereas minimal deformation is found in the footwall rocks. Hanging wall dolomites range from crush breccias (less than 5% matrix) to ultracataclasites (with 90% matrix), although cataclasites (50–70% matrix) are predominant. Foliated cataclasites occur where dolomite is thrust over shale. Progressive development of cataclastic fabrics is due to comminution by fracturing and grinding along intersecting fractures. Continued frictional grinding results in complete disruption of the original fabric to produce cataclasite and minor ultracataclasite. Grain alignment occurs by rigid body rotation with subsequent local enhancement by pressure-solution. Microstructural relations of the fault gouge suggest periodic fluctuations in fluid pressure, where λ_v (ratio of fluid to overburden pressure) probably ranged between 0.45 and 1. The Saltville thrust-sheet emplacement must have occurred in a caterpillar-like fashion involving aseismic and seismic shear. Shear stresses accompanying fault motion as determined from dolomite twin lamellae are in the order of 65 mPa.

INTRODUCTION

CONCERN about mechanisms by which thrust sheets move large distances (Smoluchowski 1909, Hubbert & Rubey 1959, Wilson 1970, Brock & Engelder 1977, Gretener 1977, Chapman 1979) has been associated with the development of thin-skinned tectonic models in foreland fold zones. Hypotheses proposed to overcome frictional resistance along major faults include abnormally high pore pressures to reduce effective normal stress (e.g. Hubbert & Rubey 1959), movement and flow in materials of low shear strength such as shale, coal and evaporites (e.g. Wilson 1970), movement on a zone sheared by pervasive cataclasis (e.g. Brock & Engelder 1977), and lubrication from frictional melt (pseudotachylyte) produced by large transient temperature increases along dry fault planes (e.g. McKenzie & Brune 1972). Microstructural characteristics of rocks in fault zones should therefore provide information on the mode of faulting and the physical conditions during movement (cf. Engelder 1974, Elliott 1976, Brock & Engelder 1977, Gretener 1977, Sibson 1977, Rutter & White 1979).

This paper investigates fault rocks along and adjacent to the Saltville thrust, a major regional thrust of the Southern Apalachian fold- and thrust-belt, U.S.A. (Fig. 1). Thrust faults of this foreland zone have linear to arcuate, discrete, discontinuous traces. These interact to produce an array of interleaved thrust-sheets. Little previous work has been done on the deformation fabrics of rocks along these faults and their mode of emplacement. Mesoscopic and microscopic fabric data of Saltville fault-rocks are presented here in an attempt to establish relationships between fault-rock fabrics, deformation mechanisms, sliding mechanisms, and physical conditions during emplacement of the Saltville thrust-sheet. Rocks were sampled from three locations along the northern section of the fault (Fig. 2). These correspond to steeply-dipping portions where dolomite occurs above the fault surface (Fig. 3).

A textural classification after Sibson (1977, table 1) is used to describe the fault-rock fabrics. This classification, however, does not allow for the possibility of foliated cataclasites, although Sibson does suggest (p. 209) that crude shape fabrics may sometimes develop during cataclastic flow. Foliated fabrics, originally thought to occur only in the quasi-plastic regime, have been recognized in the elastico-frictional regime along the Saltville thrust. The prefix term *foliated* has, therefore, been added to the cataclasite series.

FORM OF SALTVILLE THRUST

Seismic refraction studies (cf. Milici *et al.* 1979, Harris & Bayer 1979, fig. 3) indicate that the Saltville thrust has listric form and shallows with depth to merge with a master décollement within the Cambrian Rome shales (Fig. 2). Along the 690 km exposed strike-length of the fault, there are considerable variations in fault morphology and geometry. Surface dips in Virginia and Tennessee range from 0 to 50°: 10 to 30° in Tennessee (Haney 1966, Rodgers 1970); 0 to 30° at Saltville, Vir-

*Present address: Amoco Production Co., P.O. Box 50879, New Orleans, LA 70150, U.S.A.

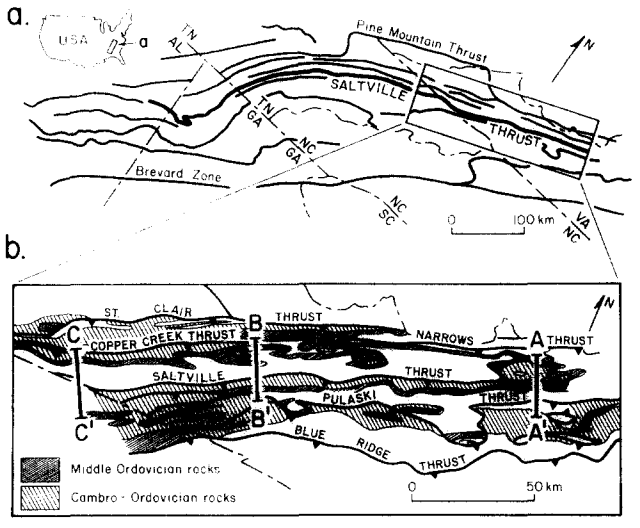

Fig. 1. Location maps. (a) Traces of major regional thrusts in the southern Appalachian foreland zone: TN, Tennessee; AL, Alabama; NC, N. Carolina; GA, Georgia; SC, S. Carolina; VA, Virginia. (b) Geology of southwest Virginia showing the sample locations and the positions of the cross-sections in Fig. 2.

ginia (Muangnoicharoen 1978, fig. 5A) and 50° at Goodwins Ferry, Virginia, Figs. 3(a) and (b). In general, the Saltville thrust has moderate to steep dips along its northern trace. The minimum total displacement along the fault in southwest Virginia is from 10 to 18 km (Dennison & Woodward 1963, fig. 3, Roeder & Witherspoon 1978, fig. 4). The estimated thickness of the thrust sheet is 4–4.5 km, whereas the present outcrop width ranges from 4 to 25 km.

Outcrop morphology of thrust

The morphology of the fault ranges from a single discrete sliding surface with minimal gouge (Fig. 3b), to a zone composed either of several discrete sliding surfaces (Fig. 3d), or of pervasive cataclasites (Figs. 3a & c). Discrete sliding surfaces are characterized by striations and chatter marks (Elliott 1976, figs. 10 and 11)

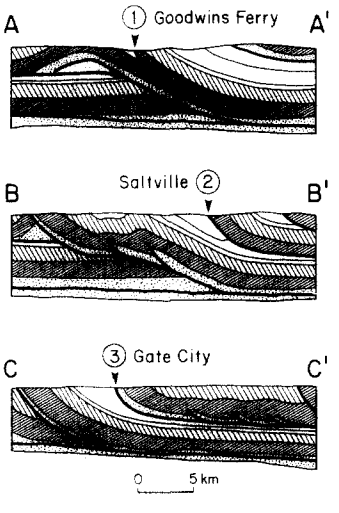

Fig. 2. Interpretative cross-sections showing the three locations where the Saltville thrust was sampled. Positions of section lines are shown in Fig. 1. Sections were modified from Butts (1933) and Milici (1970). Ornament as in Fig. 1.

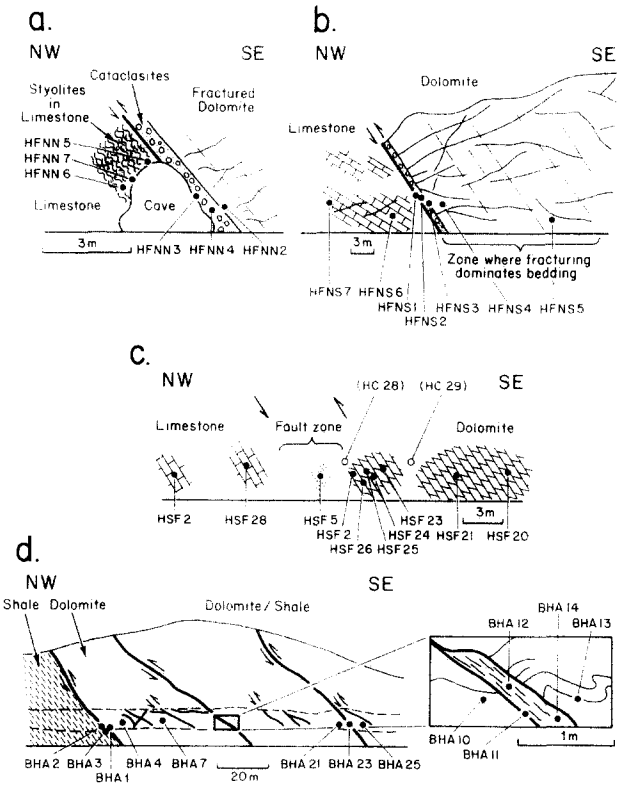

Fig. 3. Outcrop sections through the Saltville thrust at the three locations shown in Figs. 1 and 2. Dots show the sample positions in the outcrops. (a) Goodwins Ferry, Virginia: hillside outcrop at the New River Cave above Route 625 on the NE side of the New River. (b) Goodwins Ferry, Virginia: road outcrop along Route 622 on the SW side of the New River. (c) Saltville, Virginia: road outcrop on State Route 91 between Saltville and Macready. Open circles denote positions of HC 28 and HC 29 from a similar outcrop on route 107, approximately 1 km to the southwest (Mississipian Maccrady Formation shales occur in the footwall here). (d) Gate City, Virginia: road cut on State Route 23, approximately 50 m north of the Virginia–Tennessee line.

and are not normally associated with gouge. Rocks along the fault surface (cataclasites) are cohesive but less competent than surrounding rocks. Where developed, they occur in thin zones (up to 0.3 m) and are separated from surrounding lithologies by discrete surfaces (Figs. 4a–c). In some areas, however, a crude zonation is

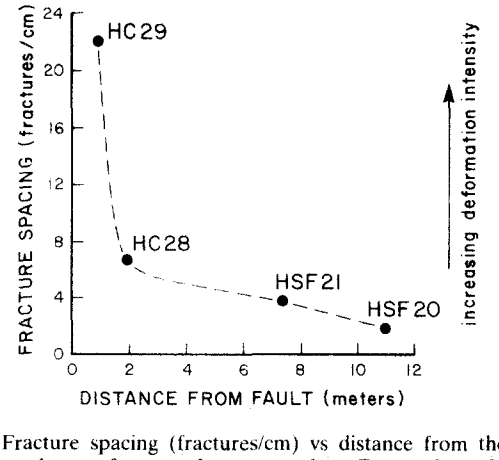

Fig. 6. Fracture spacing (fractures/cm) vs distance from the fault trace. Samples are from road outcrops along Routes 91 and 107 at Saltville, Virginia (Fig. 3c). Measurements were made from thin-section traverses. Combined traverse lengths were 12 cm for each thin section.

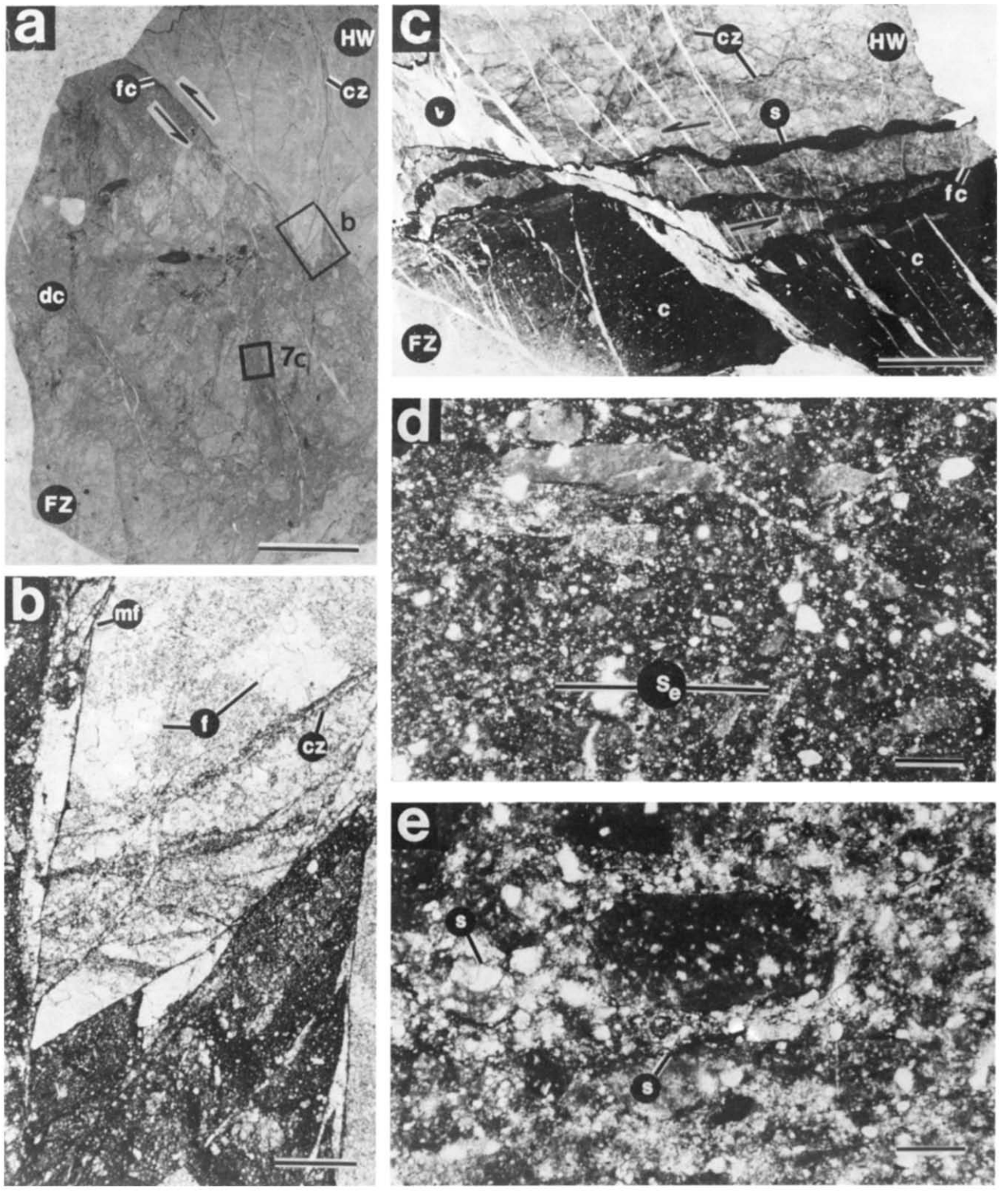

Fig. 4. Microstructural relations of the fault contact at Goodwins Ferry, Virginia (a) and (b), and Gate City, Virginia (c), (d) and (e). (a) Fractured dolomite in contact with dolomite cataclasite (HFNN2 in Fig. 3a); bar scale = 0.5 cm. (b) Enlarged portion of (a) showing the sharp nature of the fault contact with offset along a secondary cataclasite zone; bar scale = 500 μm. (c) Sharp, stylolitic fault contact between fractured dolomite and foliated cataclasite. Note the apparent offset of the veins (v) across the stylolites. (BHA 1 in Fig. 3d, bar scale = 0.5 cm). (d) (bar scale = 500 μm) and (e) (bar scale = 150 μm) are enlarged portions of the foliated cataclasite in (c) showing the foliation (S_e) defined by elongate dolomite clasts and stylolitic seams (s). (Key: fc, fault contact; HW, hanging wall; FZ, fault zone; cz, cataclasite zone; dc, dolomite cataclasite; c, foliated cataclasite; mf, microfracture; v, vein; s, stylolite).

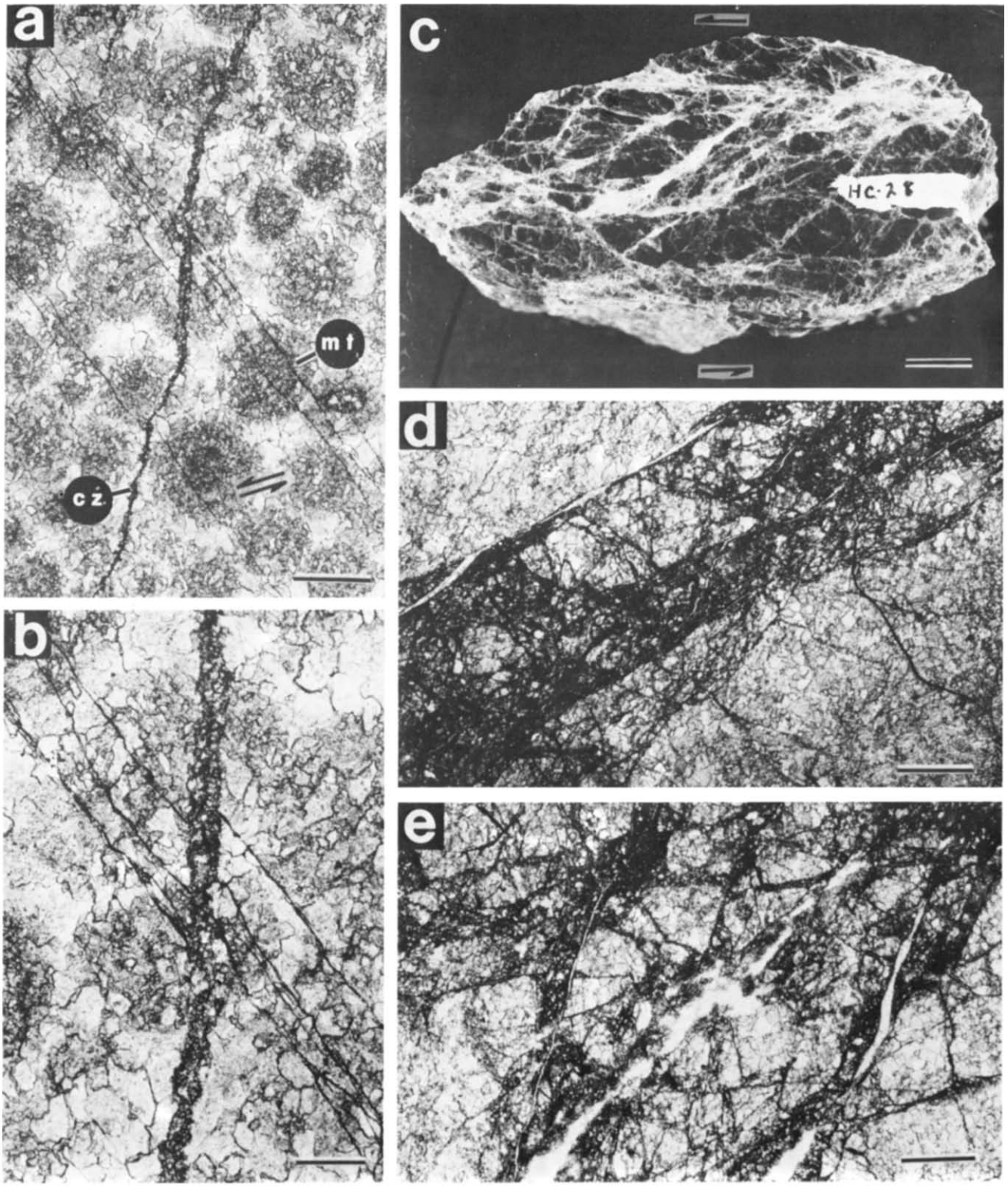

Fig. 5. Fracture patterns from Saltville localities shown in Fig. 3(c): (a) and (b) in crush breccias; (c), (d) and (e) in protocataclasite. (a) Intersecting microfractures (mf) and cataclasite zone (cz) in oolitic dolomite at HC 29, bar scale = 500 μm. Note the undeformed habit of the ooliths. (b) Enlarged portion of (a), bar scale = 150 μm. (c) Dolomite protocataclasite with intersecting cataclastic zones from HC28, bar scale = 0.5 cm. (d) Enlarged portion of a cataclastic zone in (c), bar scale = 500 μm. (e) Shatter zone due to intersecting cataclasite bands from the sample shown in (c); bar scale = 500 μm.

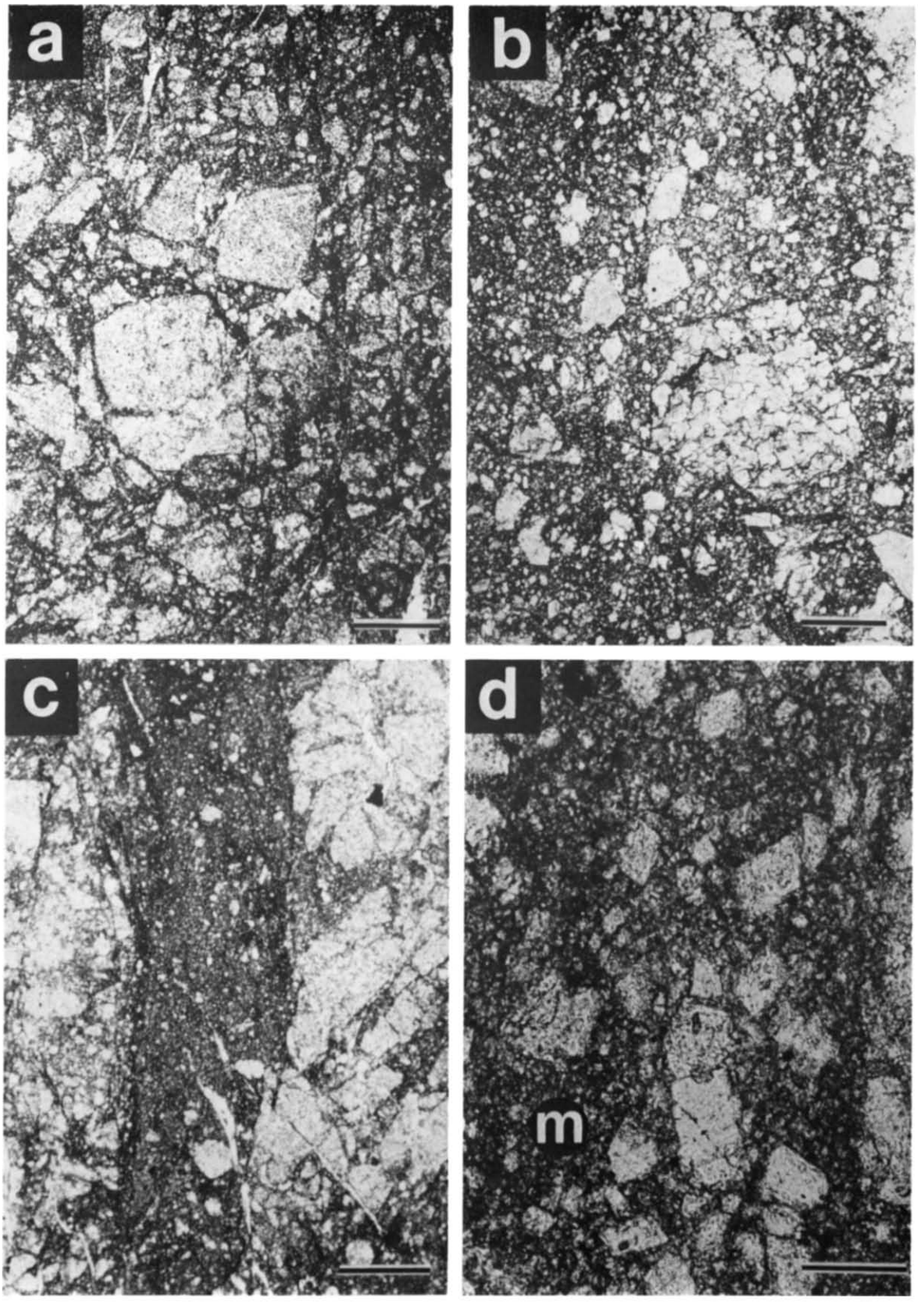

Fig. 7. Fault-rock microfabrics from Goodwins Ferry localities (Fig. 3a). (a) Non-foliated, poorly sorted cataclasite with angular clasts in a fine-grained matrix at HFNN3, bar scale = 500 μm. (b) Non-foliated cataclasite (50–70% matrix) with greater matrix proportion than (a), at HFNN4, bar scale = 500 μm. (c) Ultracataclasite zone (90–95% matrix) in cataclasite of Fig. 4(a) at HFNN2, bar scale = 500 μm. (d) Enlarged portion of the ultracataclasite showing poor sorting. m: matrix bar scale: 100 μm.

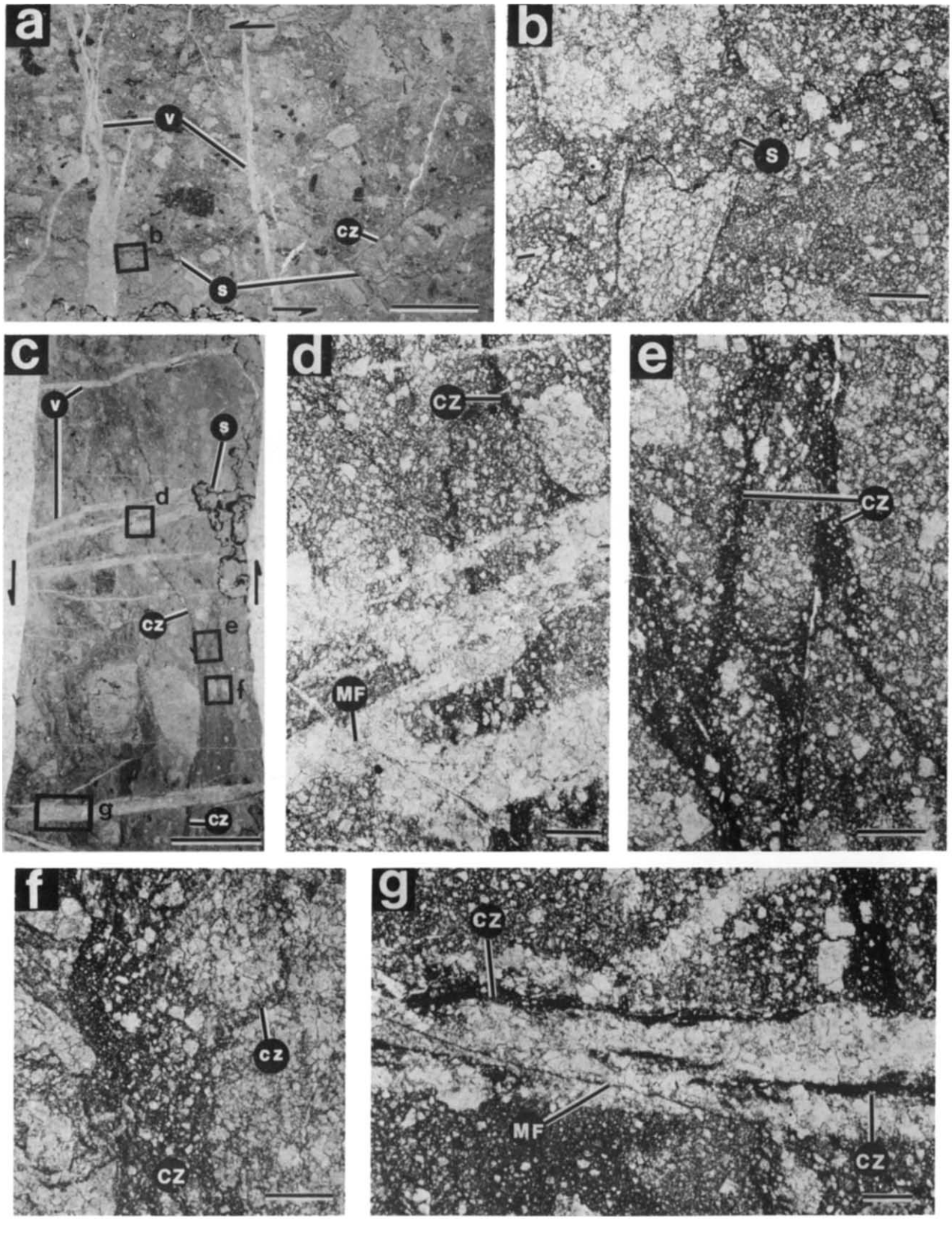

Fig. 8. Structural elements of fault rocks from cave outcrop at Goodwins Ferry, VA. (see Fig. 3a). (a) Cataclasite (HFNN3B) showing fault-parallel stylolites, fault-perpendicular veins and oblique cataclasitic zones (see Appendix) (bar scale = 0.5 cm). (b) Stylolite truncating dolomite clast; an enlarged portion of (a) (bar scale = 500 μm). (c) Cataclasite (HFNN4C) showing overprinting relations between secondary cataclasite zones, stylolites and veins (see Appendix) (bar scale = 0.5 cm). Positions of (d), (e), (f) and (g) are shown. (d) Irregular veins overprinting secondary cataclasite zones (CZ) and cut by microfractures (MF) (bar scale = 500 μm). (e) Intersecting secondary cataclasite zones (bar scale = 500 μm). (f) Cataclasite zone (CZ) with subsidiary zones (cz) responsible for increased gouge development (bar scale = 500 μm). (g) Vein cut by late stage zones of cataclasis (cz) and microfracture (bar scale = 500 μm).

evident with a gradation into fractured dolomite of the hanging wall. Thick or massive brecciated zones are absent. No basal tongues (Gretener 1977) were observed at the localities investigated.

Deformation intensity, reflected by fracturing and minor shearing (Fig. 5) decreases rapidly away from the fault (Fig. 6). A fractured zone generally occurs above the fault surface with fracturing dominant over bedding for up to 20 m. Two sets of oblique intersecting fractures, with their acute bisectrix perpendicular to the fault trace (see Figs. 3a & b) predominate. Footwall deformation is minor and varies with lithology. Shales are relatively undeformed even up to 1 m from the fault (Fig. 3d) and only show contortions in a zone up to 0.3 m thick, where dismembered folds in crumpled shale are intermixed with fragments of dolomite gouge. This grades into undeformed planar bedding fissility away from the fault. Limestones (Figs. 3a–c) are also relatively undeformed, but sometimes show increased development of bedding-parallel stylolites adjacent to the fault (Fig. 3a).

The three outcrops of the Saltville thrust which were investigated in this study show the following relationships.

(1) *Goodwins Ferry, Virginia* (*Figs. 3a & b*). Cambrian Honaker dolomites are thrust over Ordovician limestones. The fault dips 50° southeast. A thin (0.3 m wide) zone of cataclasites occurs at the dolomite–limestone interface. Minor fracturing occurs in the dolomites away from the fault surface.

(2) *Saltville, Virginia* (*Fig. 3c*). Cambrian Honaker dolomites are thrust over Mississippian limestones. The fault is poorly exposed but appears to be a zone at least 3 m wide with a dip in excess of 45° southeast. A block of cataclastic sandstone occurs within the fault zone. Minor fracturing is developed in dolomites above the fault.

(3) *Gate City Virginia* (*Fig. 3d*). Splay faults off the main Saltville thrust place a horse of dolomite (possibly Cambrian Honaker dolomite) within the Cambrian Rome Formation. The dolomite is enclosed by shale on the footwall and interbedded shale and dolomite on the hanging wall. Traces of the faults dip approximately 50° southeast. Cataclasites occur in a narrow zone (up to 0.2 m) at the dolomite–shale interface (Fig. 4c). Minor fractures occur in the dolomite away from the fault.

FAULT-ROCKS OF THE SALTVILLE THRUST

All fault-rocks are cohesive (indurated) and generally nonfoliated. Restricted largely to hanging-wall dolomites, they most commonly range from crush breccias with less than 5% matrix (Fig. 5a) to cataclasites with 50–70% matrix (Fig. 7b). Ultracataclasite (90–95% matrix) occurs along secondary shear zones in some cataclasites (Fig. 7c) but constitutes less than 2% of all the observed fault-rocks along the Saltville thrust. Clast populations are greater than 70% dolomite. Quartz clasts (chert and detrital quartz) from the original dolomite are common in some cataclasites. Limestones clasts are rare. Both foliated and nonfoliated cataclasites occur along the fault.

Nonfoliated cataclasites have a random fabric with most clasts ranging from 10 to 100 μm in diameter (Fig. 7b). Clasts have rounded to angular, elongated to rhombohedral forms with sharp, smooth to irregular grain boundaries (Figs. 7a & b). Individual clasts float in the matrix. Nonfoliated cataclasites are best developed where dolomite is thrust over limestone (Figs. 3a & b). In these rocks 90–95% of the clasts are dolomite, with 5–10% being chert.

Foliated cataclasites (Figs. 4d & e) occur where dolomite is thrust over shale (Figs. 3d and 4c). Clasts of dolomite (70%) and quartz (30%) float in a fine-grained (less than 10 μm) dolomite/clay matrix, and are 20 μm to 1.5 mm in length. The dolomite clasts commonly are more elongate than quartz and tend to show a much greater degree of preferred orientation (Fig. 4d). Quartz grains have irregular shapes and angular to subangular boundaries. The foliation is defined by both preferred orientation of elongate clasts, visible on a mesoscopic and microscopic scale, and subparallel anastomosing stylolites, visible only on a microscopic scale (Fig. 4e).

Dolomite fault-rocks

Hanging-wall dolomites have cataclasite fabrics which group into four types defined by bulk deformation characteristics and proportion of matrix (grains less than 10 μm in diameter).

Crush breccia (*e.g. Fig. 5a*). These include relatively undeformed dolomites characterized by the development of widely spaced (0.5–1.0 cm) microfractures, some of which have detectable shear displacement (Fig. 5b). Fractures and shears occur both as single surfaces and in zones, which result from the coalescing of numerous fracture and shear surfaces. Single fractures commonly form en-échelon patterns (Fig. 5b). The fractures at this stage commonly intersect one another at angles of approximately 60°. Matrix is less than 5% of the rock fabric.

Protocataclasite (*e.g. Fig. 5e*). Original microfractures form shear zones with widths up to several mm (Fig. 5d). Cataclasites with 50% matrix occur in the shear zones. However, the bulk fabric is a protocataclasite. On mesoscopic and microscopic scales, intersections of major shears are shatter zones of intense fracturing (Fig.

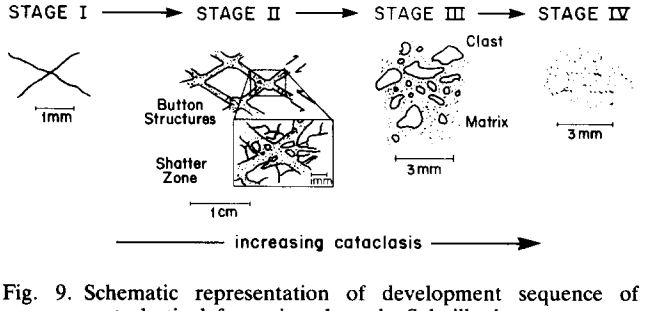

Fig. 9. Schematic representation of development sequence of cataclastic deformation along the Saltville thrust.

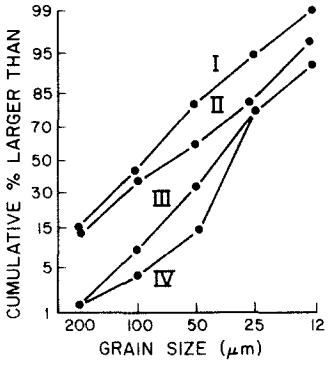

Fig. 10. Cumulative frequency curves for grainsizes of dolomite fragments in cataclasites; sample positions given in Fig. 3. I, Gate (BHA11); II, Gate City (BHA1); III, (original cataclasite) Goodwins Ferry (HFNN4C); IV, (secondary cataclasite zone) (HFNN4C). Curves are in order of increasing deformation.

5e). Button structures, diamond-shaped pods of relatively undeformed dolomite, occur between sets of intersecting shear surfaces.

Cataclasite (*e.g. Figs. 7a & b*). Original bulk fabric has been completely disrupted and button structures are not recognizable in the fault-rock fabric. Matrix constitutes 50–60% of the rock and clasts are 10 μm to several mm in diameter, although most are between 10 and 100 μm.

Ultracataclasite (*e.g. Fig. 7c*). Fabrics have more uniform grainsize with at least 90% matrix. Individual matrix grains have rounded to sub-rounded, approximately equidimensional forms, and are generally less than 10 μm in diameter, although grains up to 100 μm do occur (Fig. 7d).

Generation of the cataclasites, however, is considered progressive and sequential, as implied by the 4-stage evolution in Fig. 9. Each stage corresponds to the four categories described above. The fault zone is initially characterized by microfractures which coalesce to form conjugate shear fractures (Stage I). Above the fault, these fractures are at high angles to the fault trace (Fig. 5a), whereas in the fault zone, one set commonly parallels the fault and the other is oblique to it (Fig. 5c). Similar relations have been documented for mining induced fault zones at Boksburg, South Africa (see Gay & Ortlepp 1979, fig. 6). Stage I deformation marks the onset of cataclasis. As shearing increases, minor shear zones develop with gouge fillings (Stage II). During early phases of deformation, Stages I and II, the bulk fabric produced results in a protocataclasite upon induration due to dolomitic cementation. Progressive brittle failure leads to Stage III deformation and complete disruption of the original fabric with significant reduction in grainsize (Fig. 10). Extensive shearing and rotation of grains takes place. Continued frictional grinding and grainsize reduction produces a gouge with the matrix composition of an ultracataclasite (Stage IV).

Consistent with this deformation sequence is a continuous reduction in grainsize of dolomite fragments coupled with a changing proportion of matrix content in the fault-rock (see Fig. 10 and also compare Figs. 7a, 8f and 7c). Cumulative frequency curves I to IV show increasing effects of cataclasis; curve I (cataclasite fabric) has 82% of grains larger than 50 μm, whereas curve IV (secondary cataclasite zone of Fig. 8c) has only 15% of total grains larger than 50 μm. Furthermore the overall increase in slope from curves I to IV indicates an increase in sorting with deformation (cf. Engelder 1974, p. 1522).

Fault-rock deformation chronology

Apart from cataclastic fabrics, other textural elements in the fault zone include secondary fractures and cataclastic shears, veins and stylolites (Figs. 8a & c). Documentation of these elements in samples from the three locations investigated along the fault are given in the Appendix (see Tables A1, A2 & A3). Overprinting between them defines an approximately consistent deformation chronology for fault-rock evolution (Fig. 11). At least two stages of fracturing, veining, and gouge formation suggest cyclic development of fault-rock, although the first events (labelled 1 to 4, Fig. 11) are predominant and responsible for producing the cataclasites along the thrust. Subsequent fracturing/microshearing and gouge/breccia-formation events (labelled 5 to 6, Fig. 11) produce the intersecting zones of secondary cataclasis (Fig. 8e), but these are only minor components of the total fault-rock fabric (see Figs. 8a & c). These zones have varying orientations (see Appendix), but are predominantly parallel (Fig. 8c) or oblique (Fig. 8a) to the fault trace. Two sets are common (Fig. 8e), although three sets have been observed (see HSF 21, Table A2 in the Appendix). Minimum angles between the sets range from 50 to 90°. Displacements along secondary cataclastic zones tend to be small (less than 500 μm) and in many cases could not be detected. Induration of the cataclasite fabric prior to secondary cataclasis is inferred from the sharp contact between the zone and the host rock (Fig. 8f).

The next events (labelled 7 and 8, Fig. 11) in the development of the fault-rock microfabric involved formation of veins and stylolites (Figs. 8a–c). Local cross-cutting relations (Fig. 8a) where both veins cut stylolites and stylolites cut veins, suggest contemporaneous development of these elements. Stylolites are subparallel to the fault trace, whereas most veins are subperpendicular to the stylolites and, therefore, at large angles to the fault (Figs. 8a & c). Some veins which

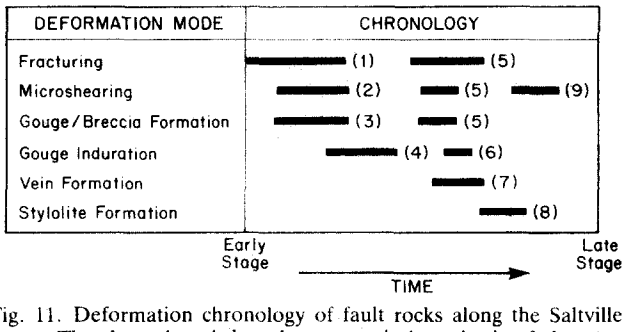

Fig. 11. Deformation chronology of fault rocks along the Saltville thrust. The chronology is based on overprinting criteria of elements listed in the Appendix.

are parallel, and others that are oblique, to the fault trace appear to have developed along the pre-existing secondary shear zones. Up to three sets of veins have been observed (see Appendix), but these do not show consistent overprinting criteria. The last event (labelled 9, Fig. 11) is minor fracturing/microshearing. Although this has produced fractures which offset veins and stylolites (Fig. 8d), the most common expression of this deformation is thin, irregular subplanar zones of cataclasis within the previously formed veins (Figs 8g).

SPECULATIONS ON SLIDING MECHANISMS

Deformation mechanisms along faults (i.e. sliding mechanisms) are affected by ambient temperature, fluid pressure, confining pressure, rock type and strain rate (Donath & Fruth 1971, Sibson 1977). Conditions which favour cataclasis correspond to those in the elastico-frictional regime (cf. Sibson 1977, p. 200), characterized by low temperatures and pressures, that is, metamorphic grades lower than greenschist facies. Both seismic and aseismic modes of failure may occur in this regime. Change from seismic to aseismic movement may be related not only to the brittle–ductile transition as suggested by Orowan (1960), but possibly also to the generation of fault gouge which enables steady state cataclastic flow (Engelder *et al.* 1975). The sliding mode during thrust emplacement is difficult to determine from deformation features along exposed ancient faults. However, fault-rock fabrics along the fault are useful in understanding deformation mechanisms and can be combined with results from experimental work to speculate on emplacement mode and conditions during thrusting. Any proposed emplacement model must account for the thickness of the fault zone and, in particular the characteristics of the gouge.

Important aspects of the Saltville thrust that need to be considered in the emplacement models include:

(1) Along its northern trace the fault generally has steep dips (up to 50°) and displays variable morphology. It ranges from a single discrete sliding surface with minimal gouge to a zone composed of several discrete sliding surfaces or of pervasive cataclasites up to 0.3 m thick.

(2) Fault-rocks are cataclasites formed by cataclasis and frictional sliding (i.e. brittle deformation) in the elastico-frictional regime.

(3) Footwall rocks, including shale and limestone, are relatively undeformed even up to 1 m from the fault.

(4) Hanging-wall rocks, generally dolomite, show a fractured zone up to 20 m above the fault surface. Fracturing and minor shearing decrease rapidly away from the fault zone and associated sliding surfaces. Maximum fracturing and gouge development are restricted to 1 m above the fault surface (see Fig. 6).

(5) Both (3) and (4) suggest that strain during fault initiation and emplacement of the thrust-sheet was localized to a narrow zone. Significant deformation of the upper plate generally did not occur.

These considerations require Saltville thrust-sheet emplacement by either abnormally high pore pressures and/or movement on a zone sheared by pervasive cataclasis. Both are associated with minimal deformation of footwall and hanging wall during thrust-sheet emplacement (Gretener 1972, 1977, Brock & Engelder 1977). Lack of pseudotachylyte along the thrust indicates that lubrication by a frictional melt did not occur. This also supports high fluid pressures and fluid movement along the fault zone, since low fluid pressures are a prerequisite for frictional melting (cf. Sibson 1980a, p. 166). The general absence of shale, coal and evaporite in the footwall immediately adjacent the fault, combined with the very minor deformation where shale was observed (Fig. 3d), suggests that flowage in weak strata was not a major factor during thrust-sheet emplacement.

Observations of hanging wall dolomite adjacent to the fault indicate that frictional sliding was important, particularly for fault initiation in dolomite, where movement was between dolomite on both upper and lower plates. In areas of minimal gouge along the fault trace, features such as striations, chatter marks and crescentic gouge marks indicate frictional wear. The general lack of fibres, accretion steps (Elliott 1976 figs. 12 and 14) and slickolites (Bretz 1940) suggests that pressure-solution slip was not important in the faulting process. Development of late stage stylolites in the gouge indicates however that pressure-solution has modified some of the cataclasite fabrics.

Generation of gouge/cataclasite along faults is also due to frictional wear. Zones of cataclasite along the Saltville thrust (Figs. 3a & 3b) could be related to: (1) repeated stress cycling associated with intermittent slip, where cyclic episodes of microcracking could develop during successive stress build-up prior to major failure (Mjachkin *et al.* 1975); (2) lower pore pressures causing higher effective stresses such that removal of asperities and production of gouge was necessary for movement and (3) the geometric need for hanging wall dolomite to accommodate bends and irregularities in the fault during movement. The lack of extensive microcracks in dolomite immediately adjacent to gouge zones (Fig. 4a) suggests that (1) is unlikely, although it may be a subsidiary mechanism facilitating gouge development in areas where cataclasite is gradational into fractured dolomite of the hanging wall. More detailed surface and subsurface investigation would be needed to substantiate (3), as the outcrops investigated precluded evaluation of this mechanism. The lack of veins in dolomite clasts within the cataclasite indicates that hydrofracturing was not important during gouge formation and places an upper constraint on the magnitude of fluid pressure. Since λ_v, the ratio of fluid pressure (P) to lithostatic load (σ_v), must be greater than 1 for hydrofracturing (Sibson 1981, p. 666), fluid pressure at the time of fault initiation in dolomite along the Saltville thrust must have been lower than lithostatic pressure. This tends to support mechanism (2).

An approximate value of λ_v at thrust initiation is 0.45, assuming an average sedimentary rock density (ϱ_r) of

2.3 g cm^{-3}, pore fluid density (ϱ_f) of 1.04 g cm^{-3} (saline water) and a depth (Z) of 5 km (see Gretener 1969, p. 257).

Other aspects which should be considered include the fracture zone above the fault and the deformation chronology shown by the fault rock microfabric. Fractured zones have been recognized above other faults (Brock and Engelder 1977, Harris & Milici 1977) and appear characteristic of thrusts in the elastico-frictional regime. Differences in orientation of fractures (compare Figs. 5a & c) with respect to the thrust trace above and within the fault zone suggest a different stress regime and possible difference in time of formation. Fractures above the fault may result from strain accommodation as the hanging wall moves over irregularities in the fault during emplacement.

Cataclasites along the fault show overprinting of secondary shear zones, stylolites and veins subsequent to development of the cataclasite fabric. Secondary shear zones have varying orientations (Figs. 8a & c) and probably reflect repeated stress cycling during thrust-sheet emplacement. Rocks along seismically-active fault zones with large finite displacement (e.g. > 1 km) must have been through the stress cycle leading to frictional failure a very large number (probably > 1000) times (Sibson pers. comm. 1981). This is somewhat problematic considering the simple textural evolution shown by the finite microfabrics of the fault-rocks (Fig. 11). In some cases however the secondary shears may represent shear bands analogous to those produced experimentally in frictional-sliding experiments (see Byerlee *et al.* 1978, fig. 6).

Overprinting criteria suggest contemporaneity of veins and stylolites in the fault zone. Veins, commonly normal to the thrust trace (Figs. 8a & d), formed under a different stress regime from the fault (compare with Sibson 1981, fig. 2a) and are probably separated in time. They are extension veins which developed by hydraulic fracturing (Secor 1965) when the fluid pressure (P) exceeded the tensile strength of the gouge. Vein fill by crystalline dolomite was probably derived from the developing fault-parallel stylolites in the matrix (see Ramsay 1980, fig. 6). The presence of the veins indicates that at the time they were generated the cataclasite was indurated, and σ_3' (effective minimum principal compressive stress) was < 0. This requires fluid pressures along the fault zone greater than the hydrostatic head. Subsequent cataclasis along these veins, and minor shear fracturing, must relate to stress build-up after dilatancy hardening. This occurs after hydro-fracturing, when fluid pressures drop towards the hydrostatic (Sibson 1981).

Such variations in fluid pressure require thrust-emplacement as a series of fast, single events as proposed by Gretener (1972, 1981). Gouge development would be associated with stress build-up during periods of low fluid pressure, and probably stick–slip behaviour (Byerlee & Brace 1968). Sliding experiments on dry, gouge-filled surfaces show both seismic and aseismic sliding modes (Jackson & Dunn 1974, Engelder *et al.* 1975). The significance of clast-preferred orientation in the foliated cataclasites is unclear. It is possible that such fabrics formed in response to slower slip and strain rates. Fast slip rates should lead to rapid dissipation of energy, an increase in local entropy and disordering of the deformation fabric (Sibson 1977), while slower slip rates could lead to a more ordered fabric.

Another important unresolved problem is the level of shear stress that accompanies motion on faults such as the Saltville thrust. Twinning within minerals, such as calcite and dolomite, can be used to infer levels of shear stress (Jamison & Spang 1976, Tullis 1980), since a critical resolved shear stress (τ_c) is necessary to produce twinning. For calcite and dolomite these are 100 and 1000 bars respectively (Jamison & Spang 1976). Analysis of twinning after Jamison & Spang (1976 fig. 4b) in hanging wall dolomites adjacent the Saltville thrust (Table 1) gives an average differential stress ($\Delta\sigma$) of 130 MPa (1300 bars) with a variation of 20 MPa (200 bars); where significant differences in $\Delta\sigma$ from different twin sets existed, the value from the highest number of twin sets was used to calculate the average. This gives a shear stress of 65 MPa (650 bars) associated with fault motion in the dolomite. Ten metres above the fault the calculated shear stress in the dolomite was 54 MPa (540 bars) (see Table 1, HSF 21). These values are higher than predicted from extrapolation of *in situ* shear stress data in hard rock (see McGarr 1980, fig. 3).

CONCLUSIONS

Fault rock fabrics may be used to determine deforma-

Table 1. Values of S_1 and $\Delta\delta$ derived from dolomite twin lamellae*

Sample	N	One set S_1	One set $\Delta\delta$	Two sets S_1	Two sets $\Delta\delta$	Structural position	Fault-rock
HFNN2	40	0.42	1190	0.345	1450	Hanging wall	microbreccia
HFNN2	71	0.40	1250			immediately adjacent	
HFNN2	81	0.35	1430	0.385	1300	to fault	
HSF21	66	0.458	1092	—	—	Hanging wall 10m	microbreccia
HSF21	27	0.465	1075	—	—	above fault	
HFNN4C	121	0.42	1190	0.385	1300	Fault zone	cataclasite
HFNN4C	44	0.42	1190	0.395	1266		

N = total number of dolomite grains inspected for twin lamellae.
*in coarse crystalline dolomite within shrinkage fenestrae (see Fig. 4b).
S_1 = resolved shear stress coefficient (see Jamison & Spang 1976, p. 870).
$\Delta\delta$ = differential stress ($\sigma_1 - \sigma_3$) in bars.

tion mechanisms and appropriate conditions during faulting and emplacement of thrust-sheets. A predominance of brittle deformation features indicates that steeply-dipping portions of the Saltville thrust, southern Appalachians, U.S.A., were emplaced in the elastico-frictional regime. Thrusting took place at depths between 5 and 8 km and temperatures below 250°C. Cataclasis and frictional wear are the primary bulk deformation mechanisms. Morphology of the Saltville thrust varies considerably and relates in part to the nature of the footwall and hanging wall lithologies. The fault is characterized both by discrete sliding surfaces with little or no gouge and by zones of cataclasite up to 0.3 m thick. Negligible deformation in footwall rocks (e.g. shale) indicates that permanent deformation during fault movement was largely confined to the fault surface or zone.

Progressive brittle failure in upper plate dolomite caused fracturing, extensive shearing, reduction in grainsize and disruption of the original fabric to produce rocks ranging from crush breccia to ultracataclasite along parts of the fault. Foliated cataclasites, which, to our knowledge have not previously been recognized along natural faults, occur along the Saltville thrust. These are defined by a preferred orientation of elongate clasts and anastomosing stylolites subparallel to the clast elongation. The foliation is thought to develop from grain rotation during cataclastic flow. Grain preferred orientation is also enhanced by pressure solution.

Microstructural relations between cataclastic fabrics, secondary cataclastic shears, veins and stylolites reflect a remarkably simple history considering potential stress cycling along major faults. Absence of early veins suggest fault initiation, and therefore, cataclasite development, occurred under low fluid pressure (possibly $\lambda_v \simeq 0.45$), whereas subsequent veins and stylolites must have been associated with $\lambda_v \rightarrow 1$. Such variations in fluid pressure may indicate that emplacement of the Saltville thrust-sheet occurred in a caterpillar-like fashion (Gretener 1972, 1981), with movement by both seismic and aseismic failure.

Analysis of twin lamellae in hanging wall dolomite gives a differential stress ($\sigma_1 - \sigma_3$) of approximately 130 MPa and a shear stress (τ) of 65 MPa accompanying motion on the Saltville thrust. Ten metres above the fault the calculated shear stress was 54 MPa. Geological evidence from the exhumed fault, therefore, indicates faulting occurred under intermediate stress conditions of Sibson (1980b, p. 6246), i.e. $10\,\text{MPa} \leqslant \tau \leqslant 100\,\text{MPa}$.

Acknowledgements—This work was completed by W.M.H. as part of the requirements for a M.S. degree at Virginia Polytechnic Institute and State University. Support was provided by a Departmental Graduate Teaching Assistantship, a Grant-in-Aid of Research from Sigma Xi (The Scientific Research Society of North America), and research grants from the Geological Society of America and the American Association of Petroleum Geologists, all awarded to W.M.H. Partial summer support was from National Science Foundation Grant No. EAR. 79-19703 awarded to D.R.G.

The authors would like to thank W. D. Lowry and J. F. Read for their comments on the manuscript during thesis preparation, and Rick Sibson, Terry Engelder and Robert Simon for their incisive criticisms which greatly improved the manuscript. Assistance for paper preparation was given by V.P.I. & S.U.; thanks are extended to Martin Eiss, Sharon Chiang and Eric Raitch for drafting, Donna Williams and Hersha Evans-Wardell for typing, and Cynthia Zauner and Llyn Sharp for photography.

REFERENCES

Bretz, J. H. 1940. Solution cavities in the Joliot Limestone of northeast Illinois. *J. Geol.* **48,** 337–384.

Brock, W. C. & Engelder, T. 1977. Deformation associated with the movement of the Muddy Mountain overthrust in the Buffington Window, southeastern Nevada. *Bull. geol. Soc. Am.* **88,** 1667–1677.

Butts, C. 1933. Geologic map of the Appalachian Valley of Virginia with explanatory text. *Va. Geol. Surv. Bull.*, 42, map.

Byerlee, J. D. & Brace, W. F. 1968. Stick-slip stable sliding and earthquakes, part 1. Effect on rock type, pressure, strain rate and stiffness. *J. geophys. Res.* **73,** 6031–6037.

Byerlee, J. D., Myachkin, V., Summers, R. & Voeroda, O. 1978. Structures developed in fault gouge during stable sliding and stick-slip. *Tectonophysics* **44,** 161–171.

Chapman, R. E. 1979. Mechanics of unlubricated sliding. *Bull. geol. Soc. Am.* **90,** 19–28.

Dennison, J. M. & Woodward, H. P. 1963. Palinspastic maps of central Appalachians. *Bull. Am. Ass. Petrol. Geol.* **47,** 666–680.

Donath, F. A. & Fruth, L. S. 1971. Dependence of strain rate effects on deformation mechanisms and rock type. *J. Geol.* **79,** 347–371.

Elliott, D. 1976. The energy balance and deformation of thrust sheets. *Phil. trans. R. Soc. Lond.* **283A,** 289–312.

Engelder, J. T. 1974. Cataclasis and the generation of fault gouge. *Bull. geol. Soc. Am.* **85,** 1515–1522.

Engelder, J. T., Logan, J. M., & Handin, J. 1975. The sliding characteristics of sandstone on quartz fault gouge. *Pageoph.* **113,** 70–86.

Gay, N. C. & Ortlepp, W. D. 1979. Anatomy of a mining induced fault zone. *Bull. geol. Soc. Am.* **90,** 47–58.

Gretener, P. E., 1969. Fluid pressure in porous media—its importance in geology: a review. *Bull. Can. Petrol. Geol.* **17,** 255–295.

Gretener, P. E. 1972. Thoughts on overthrust faulting in a layered sequence. *Bull. Can. Petrol. Geol.* **20,** 583–607.

Gretener, P. E. 1977. On the character of thrust faults with particular reference to the basal tongues. *Bull. Can. Petrol. Geol.* **25,** 110–122.

Gretener, P. E. 1981. Pore pressure, discontinuities, isostasy, and overthrusts. In: *Thrust and Nappe Tectonics* (edited by McClay, K. R. & Price, N. J.) *Specs. Publs geol. Soc. Lond.* **9,** 33–39.

Haney, D. C. 1966. Structural geology along a segment of the Saltville fault, Hawkins County, Tennessee. Unpublished Ph.D. dissertation, University of Tennessee, Lexington.

Harris, L. D. & Milici, R. C. 1977. Characteristics of thin-skinned style of deformation in the southern Appalachians and potential hydrocarbon traps. *Prof. Pap. U. S. geol. Surv.* **1018,** 1–40.

Harris, L. D. & Bayer, K. C. 1979. Sequential development of the Appalachian orogen above a master decollement — a hypothesis. *Geology* **7,** 568–572.

Hubbert, M. K. & Rubey, W. W. 1959. Role of fluid pressure in mechanics of overthrust faulting. *Bull. geol. Soc. Am.* **70,** 115–166.

Jackson, R. E. & Dunn, D. E. 1974. Experimental sliding function and cataclasis of foliated rocks. *Int. J. Rock Mech. Min. Sci.* **11,** 235–249.

Jamison, W. R. & Spang, J. H. 1976. Use of calcite twin lamellae to infer differential stress. *Bull. geol. Soc. Am.* **87,** 868–872.

McGarr, A. 1980. Some constraints on levels of shear stress in the crust from observations and theory. *J. geophys. Res.* **85,** 6231–6238.

McKenzie, D. & Brune, J. N. 1972. Melting on fault planes during large earthquakes. *Geophys. J. R. ast. Soc.* **29,** 65–078.

Milici, R. C. 1970. The Allegheny structural front in Tennessee and its regional tectonic implications. *Am. J. Sci.* **268,** 127–141.

Milici, R., Harris, L. D. & Statler, A. T. 1979. An interpretation of seismic cross sections in the Valley and Ridge of eastern Tennessee. *Tenn. Div. Geology, Oil and Gas Seismic Investigations Series* **1,** 2 sheets.

Mjachkin, V. I., Brace, W. F., Sobolev, G. A. & Dieterich, J. H. 1975. Two models for earthquake fore runners. *Pure appl. Geophys.* **113,** 169–181.

Muangnoicharoen, N. 1978. The Saltville thrust decollement — deformation of the Mccrady Formation evaporites. Unpublished Ph.D. dissertation, University of North California at Chapel Hill.

Orowan, E. 1960. Mechanisms of seismic faulting. *Mem. geol. Soc. Am.* **79,** 323–345.

Ramsay, J. G. 1980. The crack-seal mechanism of rock deformation. *Nature, Lond.* **284,** 135–139.
Roeder, D. & Witherspoon, W. D. 1978. Palinspastic map of east Tennessee. *Am. J. Sci.* **278,** 543–550.
Rutter, E. H. & White, S. H. 1979. The microstructures and rheology of fault gouges produced experimentally under wet and dry conditions at temperatures up to 400°C. *Bull. Mineral.* **102,** 101–109.
Secor, D. T. 1965. Role of fluid pressure in jointing. *Am. J. Sci.* **263,** 633–646.
Sibson, R. H. 1977. Fault rocks and fault mechanisms. *J. geol. Soc. Lond.* **133,** 191–213.
Sibson, R. H. 1980a. Transient discontinuities in ductile shear zones. *J. Struct. Geol.* **2,** 165–171.
Sibson, R. H. 1980b. Power dissipation and stress levels on faults in the upper crust. *J. geophys. Res.* **85,** 6239–6247.
Sibson, R. H. 1981. Controls on low stress hydro-fracture dilantancy in thrust, wrench and normal fault terrains. *Nature, Lond.* **289,** 665–667.
Smoluchowski, M. S. 1909. Some remarks on the mechanics of overthrusts. *Geol. Mag.* **6,** 204–205.
Tullis, T. E. 1980. The use of mechanical twinning in minerals as a measure of shear stress magnitudes. *J. geophys. Res.* **85,** 6263–6268.
Wilson, R. C., Jr. 1970. The mechanical properties of the shear zone of the Lewis overthrust, Glacier National Park, Montana. Unpublished Ph.D. dissertation, Texas A & M Univ., College Station.

APPENDIX

Fault-rock microstructural data

Key: N, orientation normal to fault; P, orientation parallel to fault; O, orientation oblique to fault; (60°), min. angle between oblique sets in thin section; [30°] angle between shear and fault zone boundary in thin section (cataclastic shears, stylolites, veins); d, dextral movement sense; s, sinistral movement sense; n, no detectable offset; *, dominant set (cataclastic shears).

Table A1. Outcrops at Goodwins Ferry, VA (see Figs. 3a & b)

Sample	Gouge	Cataclastic shears	Stylolites	Veins	Cataclastic shears	Lithology	Position	Fault-rock type
HFNN6			one set O[60°]	three sets O[30°], N and P.	two fracture sets On, On (60°)	limestone	footwall (1.2 m below fault)	undeformed
HFNN7				three sets: P, O[10°] O[30°]		limestone	footwall (1 m below fault)	relatively undeformed
HFNN5			two sets: P, N	two sets: N, O[80°]	along O veins	limestone	footwall (0.2 m below fault)	relatively undeformed
HFNN3B	——	two sets: Pn*, On (50°)	P	N	along P veins	dolomite	fault zone	cataclasite
HFNN4A	——	two sets: Pd, Od (50°)	P	N	along P veins	dolomite	fault zone	cataclasite
HFNN4C	——	two sets:	P	N		dolomite	fault zone	cataclasite
HFNN2	——	complex network				dolomite	upper boundary of fault	cataclasite
		3 sets: Ps, Od, Od				dolomite	hanging wall	microbreccia
HFNS4B				Stylolites	three sets Pn*, O[70°], On[50°]	dolomite	hanging wall (0.2 m above fault)	microbreccia to protocataclasite

Table A2. Outcrop at Saltville, VA (see Fig. 3c)

Sample	Gouge	Cataclastic shears	Stylolites	Veins	Cataclastic shears	Lithology	Position	Fault-rock type
HSF2			normal to bedding (weak)			limestone	footwall (10 m below fault)	undeformed
HSF28			normal to bedding (weak)	N (minor)		calcareous sandstone	footwall (6 m below fault)	undeformed
HSF6A		two sets: Os, On (70°)				sandstone	fault zone	crush microbreccia
HSF24			2 sets O, O (80°)			algal dolomite	hanging wall (2 m above fault	relatively undeformed
HSF21		three sets Pn, O [58], O [90°]		two sets: P, O	along P veins	dolomite	hanging wall (10 m above fault)	crush microbreccia
HSF20		two sets Od, On (60–70°)		along cataclastic shears	1 set of fractures P	dolomite	hanging wall (13 m above fault)	crush microbreccia
HC28		two main sets: Pn*, On (60°)				dolomite	fault contact	protocataclasite
HC29		two equal sets: Ox, On (60 irregular)				dolomite	hanging wall (5 m from fault)	crush microbreccia

Table A3. Outcrop at Gate City, VA (Fig. 3d)

Sample	Gouge	Cataclastic shears	Stylolites	Veins	Cataclastic shear zones	Lithology	Position	Fault-rock type
BHA2	——		P (minor)	N	along veins	shale	footwall on fault plane	Cataclasite
BHA3	——		P (minor)	irregular N	two sets On, On (90°)	shale	fault zone	cataclasite
BHA1C		(complex) two sets: Od, (90°)		two sets: O, O (20°)		dolomite	hanging wall (adjacent fault)	microbreccia to protocataclasite
BHA1B	——	two sets: Pa, On dolomite	P	3 sets P, O [20°] and Nn		dolomite and shale	fault contact	protocataclasite to cataclasite
BHA4			P (minor)			dolomite	hanging wall (8 m above fault)	microbreccia
BHA10		complex				dolomite	footwall (adjacent fault)	microbreccia to protocataclasite
BHA11	——		P	N (minor)		dolomite	fault zone	cataclasite
BHA12		two sets Os*, On (60°)				dolomitic sandstone	fault zone	microbreccia